

Model Building of Metal Oxide Surfaces and Vibronic Coupling Density as a Reactivity Index: Regioselectivity of CO₂ Adsorption on Ag-loaded Ga₂O₃

Yasuro Kojima¹, Wataru Ota^{1,2}, Kentaro Teramura^{1,3}, Saburo Hosokawa^{1,3}, Tsunehiro Tanaka^{1,3},
Tohru Sato^{1,2,3*}

¹ *Department of Molecular Engineering, Graduate School of Engineering, Kyoto University,
Nishikyo-ku, Kyoto 615-8510, Japan*

² *Fukui Institute for Fundamental Chemistry, Kyoto University, Sakyo-ku,
Kyoto 606-8103, Japan*

³ *Unit of Elements Strategy Initiative for Catalysts & Batteries, Kyoto University, Nishikyo-ku,
Kyoto 615-8510, Japan*

(Dated: August 23, 2018)

Abstract

The step-by-step hydrogen-terminated (SSHT) model is proposed as a model for the surfaces of metal oxides. Using this model, it is found that the vibronic coupling density (VCD) can be employed as a reactivity index for surface reactions. As an example, the regioselectivity of CO₂ adsorption on the Ag-loaded Ga₂O₃ photocatalyst surface is investigated based on VCD analysis. The cluster model constructed by the SSHT approach reasonably reflects the electronic structures of the Ga₂O₃ surface. The geometry of CO₂ adsorbed on the Ag-loaded Ga₂O₃ cluster has a bent structure, which is favorable for its photocatalytic reduction to CO.

* Corresponding author at: Fukui Institute for Fundamental Chemistry, Kyoto University, Takano Nishihiraki-cho 34-4 Sakyo-ku, Kyoto 606-8103, Japan.

Email address: tsato@scl.kyoto-u.ac.jp

1 Introduction

Heterogeneous catalysis, particularly for reactions between molecules and solid surfaces, has been extensively studied [1]. To design heterogeneous catalysts and understand of their mechanisms, the sites for molecular adsorption on the solid catalyst must be clarified. The adsorption sites can be predicted theoretically by finding the position of a molecule on a surface that has the lowest energy of all possible positions on the surface. However, it is impractical to calculate all the energies because, in general, there are many adsorption sites for a molecule on a solid surface. Therefore, a reactivity index to predict the adsorption sites based only on the information of solid surface is desirable.

Previously, we identified the regioselectivity of cycloaddition to fullerene [2–4], metallofullerene [5], and large polycyclic aromatic hydrocarbons [6] using the vibronic coupling density (VCD) as the reactivity index. Vibronic coupling, the coupling between electron and nuclear vibrations, stabilizes a system by structural relaxation after charge transfer. The VCD as a function of a position identifies the reactive sites as those where the vibronic coupling is large. It is expected that the VCD can be utilized as a reactivity index for systems with various reactive sites, such as solid surfaces.

β -Ga₂O₃ is a heterogeneous catalyst that reduces CO₂ to CO using H₂ as a reductant under photoirradiation [7,8]. The selectivity of CO₂ reduction is increased by modifying β -Ga₂O₃ with Ag, which acts as a cocatalyst [9–13]. H₂O, which is abundant, is used as the reductant in the Ag-loaded Ga₂O₃ system. In this study, we applied VCD to the Ag-loaded Ga₂O₃ surface to show the effectiveness of VCD as a reactivity index for CO₂ adsorption on the surface. This is the first report of the application of VCD to a solid surface and could provide the basis for extending the applicability of VCD to solid surfaces in general.

Reactivity indices, such as the frontier orbital density or VCD, strongly depend on the electronic structure of the frontier level. When building a model for the surface reactions of metal oxides based on a bulk crystal structure, the treatment of dangling bonds strongly affects the electronic structure. For instance, because hydrogen termination for dangling bonds involves electron doping, the frontier level is shifted by hydrogen termination. In this study, to build a model for the subsequent calculations, we employed a step-by-step hydrogen-terminated (SSHT) approach to reproduce the experimental observations.

In Sec. 2, we describe the theory of vibronic coupling. In Sec. 3, we describe the computational methods. In Sec. 4.1, we present a method to build a cluster model of the Ag-loaded Ga₂O₃ surface by the SSHT approach. In Sec. 4.2, we investigate the regioselectivity of CO₂ adsorption on Ag-loaded Ga₂O₃ cluster using VCD as the

reactivity index. Finally, in Sec. 5, we present the conclusions of this study.

2 Theory

In the early stage of chemical reactions, charge transfer occurs between reactants by intermolecular orbital interactions. Following charge transfer, the system is further stabilized by intramolecular deformation. This structural relaxation is induced by vibronic coupling. The vibronic coupling constant (VCC) V , which quantitatively evaluates the strength of vibronic couplings, is defined by [14, 15]

$$V = \left(\frac{\partial E_{\text{CT}}}{\partial \xi} \right)_{\mathbf{R}_0}, \quad (1)$$

where E_{CT} is the total energy of the charge-transfer state, and \mathbf{R}_0 is the equilibrium geometry before charge transfer. ξ is the reaction coordinate along the nuclear vibration that gives the largest vibronic coupling

$$\xi = \sum_{\alpha} \frac{V_{\alpha}}{\sqrt{\sum_{\alpha} |V_{\alpha}|^2}} Q_{\alpha}, \quad (2)$$

where Q_{α} is a normal coordinate and V_{α} is the VCC of vibrational mode α .

The VCD η is provided by the integrand of the VCC,

$$V = \int d^3\mathbf{r} \eta(\mathbf{r}). \quad (3)$$

Since $\eta(\mathbf{r})$ is a function of the spatial coordinate \mathbf{r} , $\eta(\mathbf{r})$ gives the local information about the VCC. The VCD can be divided into electronic and vibrational contributions:

$$\eta(\mathbf{r}) = \Delta\rho(\mathbf{r}) \times v(\mathbf{r}). \quad (4)$$

$\Delta\rho(\mathbf{r})$ is the electron density difference between neutral and charge-transfer states, and $v(\mathbf{r})$ is the potential derivative defined as the derivative of the potential acting on an electron from all the nuclei u with respect to ξ . The total differential of the chemical potential $\mu = \mu[N; u]$ which is a functional of the number of electrons N and u is given by [14]

$$d\mu = 2\zeta dN + \int \eta(\mathbf{r}) d\xi d^3\mathbf{r}, \quad (5)$$

where ζ is the absolute hardness. In terms of the chemical reactivity theory proposed by R. G. Parr and W. Yang [16, 17], the preferred direction for a reagent approaching a species is the one for which the initial $|d\mu|$ is the maximum. The first term on the right-hand side of Eq. (5) is less direction sensitive than the second term. Thus, the preferred direction can be said to be that for which the $\eta(\mathbf{r})$ of a species is a maximum.

3 Computational method

For the calculations of the VCC and VCD, we first optimized the geometry of a neutral Ag-loaded Ga_2O_3 cluster and performed a vibrational analysis. Then, we calculated the forces acting on the nuclei for the neutral optimized structure in a cationic state. The charge-transfer state was chosen to be a cationic state because we assume that an electron is transferred from the Ag-loaded Ga_2O_3 surface to CO_2 in the reduction of CO_2 . Finally, we determined the adsorbed structure of CO_2 on the Ag-loaded Ga_2O_3 cluster by geometry optimization. The computational level was set at the B3LYP/6-31G(d,p) level for the Ga, O, and H atoms and at the B3LYP/LANL2TZ level for the Ag atom. The core electrons in the Ag atom were replaced by effective core potentials. These calculations were performed using GAUSSIAN 09 [18,19]. The VCC and VCD were calculated using our own code.

4 Results

4.1 Cluster model of Ag-loaded Ga_2O_3 surface

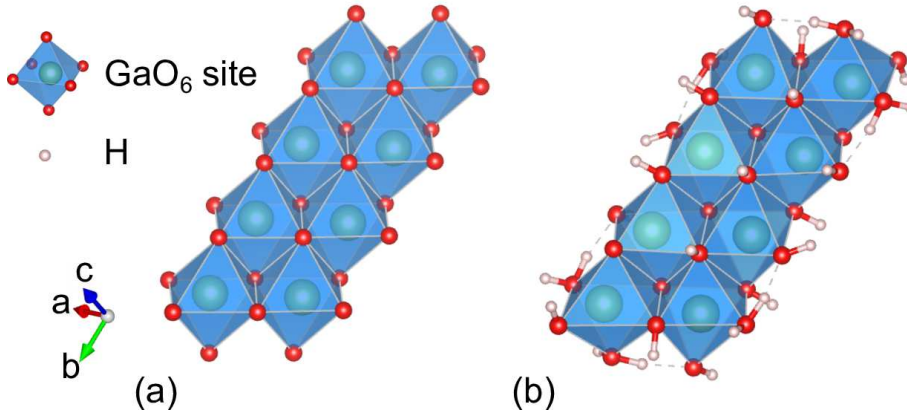


Figure 1: Structures of the (a) bare and (b) SSHT model for the Ga_2O_3 surface where Ga atoms are located at the octahedral sites formed by O atoms.

$\beta\text{-Ga}_2\text{O}_3$ consists of Ga atoms located at the octahedral and tetrahedral sites formed by O atoms [20,21], as illustrated in Figure S1 in the Supplementary Material. The octahedra share edges whereas the tetrahedra share corners in the b -axis direction. The tetrahedra also share corners with the octahedra. We expected that the electrons used for the reduction of CO_2 migrate through the octahedra shared edges. In this study, eight adjacent octahedral sites are employed as a bare cluster model of the $\beta\text{-Ga}_2\text{O}_3$ surface (Figure 1 (a)).

Figure 2 shows the calculated orbital levels of the bare cluster. The band gap of $\beta\text{-Ga}_2\text{O}_3$ has been experimen-

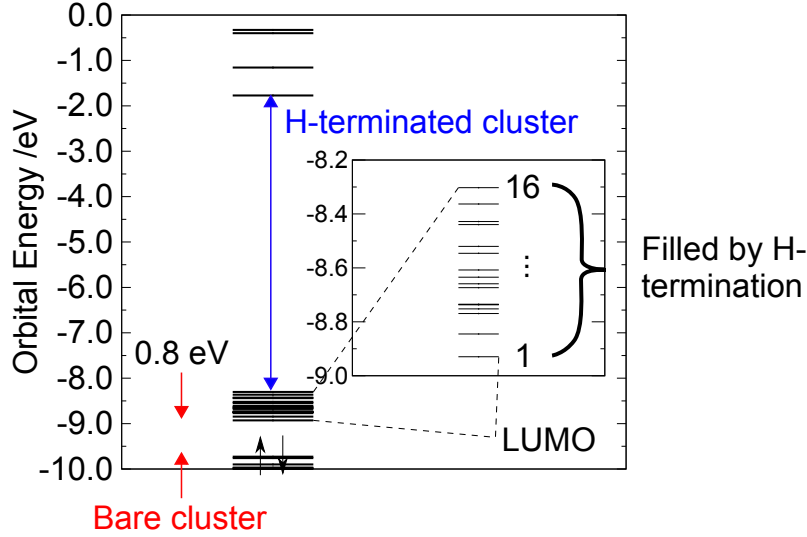


Figure 2: Orbital levels of the bare cluster with an energy gap of 0.8 eV. Dangling bonds at the O atoms are terminated with H atoms until the cluster model has an energy gap that agrees with the experimental value.

tally estimated to be 4.6 eV [11]. However, the energy gap of the bare cluster is 0.8 eV, which is much smaller than the experimental value. This is because the occupied molecular orbitals become unoccupied when the cluster is cut from the crystal structure. The bare cluster has reactive dangling bonds arising from the cleavage of O atoms. The dangling bonds at the O atoms are terminated by H atoms because it has been experimentally observed that H atoms are adsorbed on the Ga_2O_3 surface [8]. The hydrogen termination, which involves electron doping, shifts the frontier level. The 16 unoccupied molecular orbitals must be occupied for the model to have a reasonably wide energy gap. Thus, the 32 H atoms, i.e., 2 H atoms for each unoccupied molecular orbital, are step-by-step bonded to O atoms with large molecular orbital coefficients. As a result, we obtained the hydrogen-terminated cluster with an energy gap of 5.4 eV after geometry optimization. Figure S2 in the Supplementary Material shows in detail the process of step-by-step hydrogen termination. Hereafter, we refer to this hydrogen terminated cluster as the SSHT model for the Ga_2O_3 surface. Figure 1 (b) shows the optimized structure of the SSHT model.

The diffuse reflectance spectrum of the SSHT cluster model is evaluated to examine its reliability. The spectrum $g(x)$, which depends on the absorption energy x , is calculated from the oscillator strengths multiplied by the Gaussian distribution function,

$$g(x) = \sum_{i=1}^{10} \frac{f_i}{\sqrt{2\pi\sigma^2}} \exp\left(-\frac{(x-u_i)^2}{2\sigma^2}\right), \quad (6)$$

where f_i is the oscillator strength of a transition from S_0 to the Franck–Condon S_i states, and u_i is the excitation energy from S_0 to the Franck–Condon S_i states. The value of i is restricted between 1 and 10. The values of f_i and u_i were calculated using time-dependent density functional theory. Here, σ^2 is the variance of the Gaussian

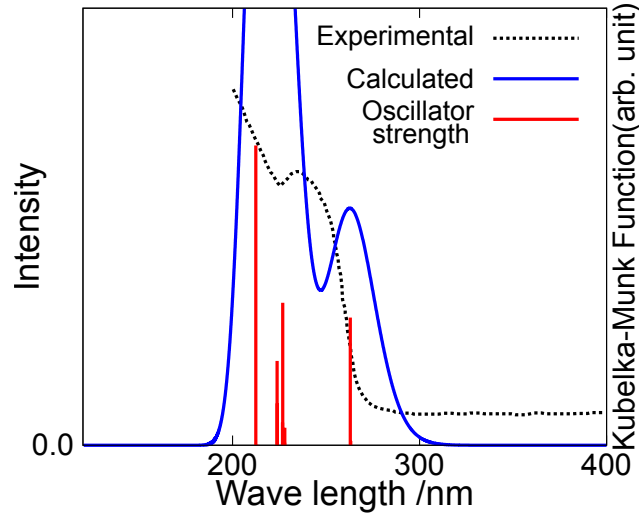


Figure 3: Experimental (black dotted line) [11] and calculated (blue line) diffuse reflectance spectra. The red lines represent calculated oscillator strengths.

distribution function and was set to 0.05 eV^2 . Figure 3 shows a comparison of the experimental and calculated diffuse reflectance spectrum [11]. Although the calculated spectrum is shifted to the long-wavelength region with respect to the experimental spectrum, the two peaks of the calculated spectrum at 219 and 263 nm are also observed experimentally. Thus, the SSHT cluster is suitable for use as a model for the Ga_2O_3 surface.

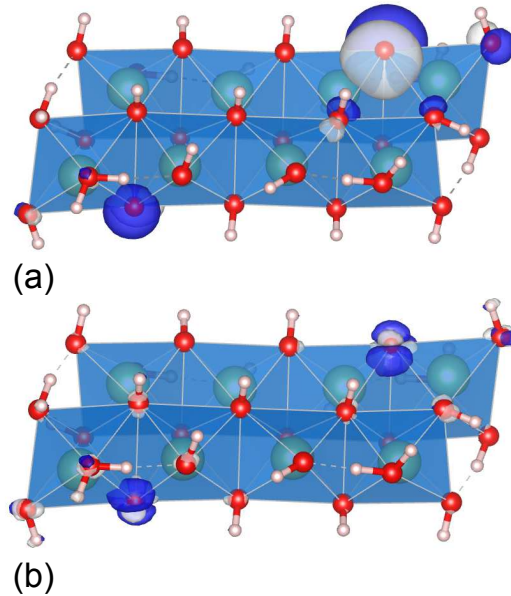


Figure 4: (a) HOMO and (b) VCD $\eta(\mathbf{r})$ of the SSHT cluster model for the Ga_2O_3 surface. The HOMO and VCD are localized on the O atoms where H atoms are not bonded. The isosurface values of HOMO and VCD are 3.0×10^{-2} and 2.5×10^{-5} a.u., respectively.

It should be noted that, in the SSHT cluster model, H atoms are not bonded to all O atoms, although all the dangling bonds are terminated by H atoms. There are 20, 6, and 2 O atoms with which 1, 2, and 0 H atoms are bonded, respectively. The O atoms without hydrogen termination have a pair of electrons, and, thus, act as Lewis bases. This is supported by the highest occupied molecular orbital (HOMO) of the SSHT cluster model, as shown in Figure 4 (a), which is strongly localized on the O atoms without hydrogen termination. This result indicates that these O atoms donate electrons to the reactants. The HOMO is doubly degenerate because the Lewis basic O atoms are located at both the front and back surfaces of the SSHT cluster model. Figure 4 (b) shows the VCD of the SSHT cluster model, which is also localized on the O atoms without hydrogen termination. The stabilization arising from the structural relaxation after charge transfer is large at the sites where the VCD is localized. Therefore, the Ag-loaded Ga_2O_3 surface is modeled by placing a single Ag atom on one of the Lewis basic O atoms in the SSHT cluster model. The Cartesian coordinates of the SSHT cluster model for the Ga_2O_3 and Ag-loaded Ga_2O_3 surfaces are given in Tables S1 and S2 of the Supplementary Material.

4.2 Regioselectivity of CO_2 adsorption on Ag-loaded Ga_2O_3 cluster

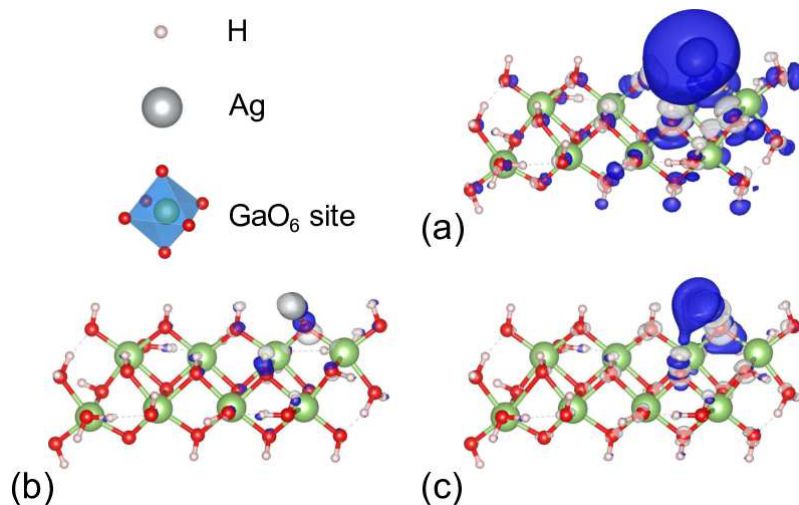


Figure 5: (a) The electron density difference $\Delta\rho(\mathbf{r})$, (b) potential derivative $v(\mathbf{r})$, and (c) VCD $\eta(\mathbf{r})$ of the Ag-loaded Ga_2O_3 cluster. The isosurface values of $\Delta\rho(\mathbf{r})$, $v(\mathbf{r})$, and $\eta(\mathbf{r})$ are 10^{-3} , 10^{-2} , and 10^{-5} a.u., respectively.

Figure 5 shows the electron density difference $\Delta\rho(\mathbf{r})$, the potential derivative $v(\mathbf{r})$, and the VCD $\eta(\mathbf{r})$ of the Ag-loaded Ga_2O_3 cluster. Here, $\Delta\rho(\mathbf{r})$, the electron density difference between the neutral and cationic states, is delocalized around the Ag atom because the electron is mainly extracted from the Ag atom. $v(\mathbf{r})$ is large at the Ag and adjacent O atoms. Consequently, $\eta(\mathbf{r})$, which is given by the product of $\Delta\rho(\mathbf{r})$ and $v(\mathbf{r})$, is localized on the

Ag atom as well as on the O atoms located near the Ag atom. Since $\eta(\mathbf{r})$ is distributed over the Ag atom and the O atoms at the surface of the Ga_2O_3 cluster, structural relaxation occurs between the Ag atom and the Ga_2O_3 cluster following charge transfer. This result implies that catalytic activity depends on the type of solid surface on which the Ag atom is loaded.

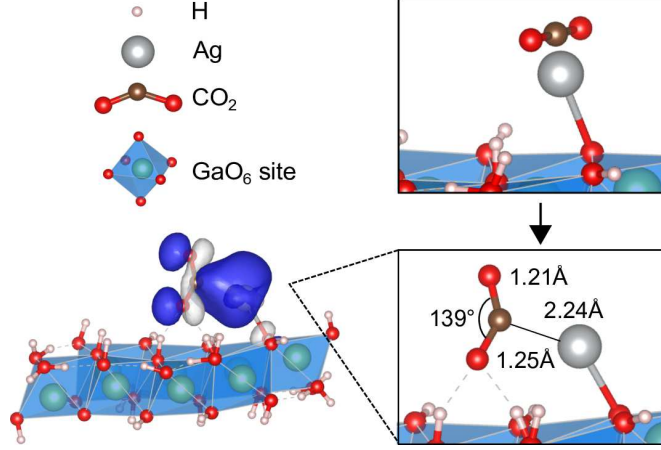


Figure 6: Optimized structure and HOMO of CO_2 on the Ag-loaded Ga_2O_3 cluster. The HOMO mainly consists of LUMO for bent CO_2 and Ag s orbitals. The isosurface value is 0.03 a.u.

Geometry optimization is performed after the initial position of CO_2 is set above the Ag atom, as shown in Figure 6. The adsorbed structure of CO_2 is found to have an O-C-O angle of 139° and O-C distances of 1.21 and 1.25 Å. The adsorbed structure is obtained in the region where the VCD is localized. The adsorption energy of CO_2 E_{ad} is defined by

$$E_{\text{ad}} = E_{\text{CO}_2} + E_{\text{cluster}} - E_{\text{CO}_2/\text{cluster}}, \quad (7)$$

where E_{CO_2} , E_{cluster} , and $E_{\text{CO}_2/\text{cluster}}$ are the energies of isolated CO_2 , isolated Ag-loaded Ga_2O_3 cluster, and CO_2 on the cluster, respectively. The E_{ad} of CO_2 is calculated to be 0.58 eV, indicating that the CO_2 with a bent structure is favorably adsorbed on the Ag-loaded Ga_2O_3 cluster.

The reduction of CO_2 to CO is favored when the LUMO level of CO_2 is low [22] because electrons are transferred from the Ag-loaded Ga_2O_3 surface to CO_2 for the reduction of CO_2 . Figure 7 shows the frontier orbital levels of CO_2 with a linear structure and the structure extracted from Figure 6. The LUMO level of bent CO_2 is lower than that of the linear structure although bent CO_2 is energetically unstable. Thus, the Ag-loaded Ga_2O_3 surface on which bent CO_2 can be favorably adsorbed is suitable for CO_2 reduction. As shown in Figure 6, the HOMO of CO_2 on the Ag-loaded Ga_2O_3 cluster is similar to the LUMO of bent CO_2 and Ag s orbitals, leading to charge transfer from the Ag-loaded Ga_2O_3 cluster to CO_2 . The natural charges of the Ag atom are found to change from

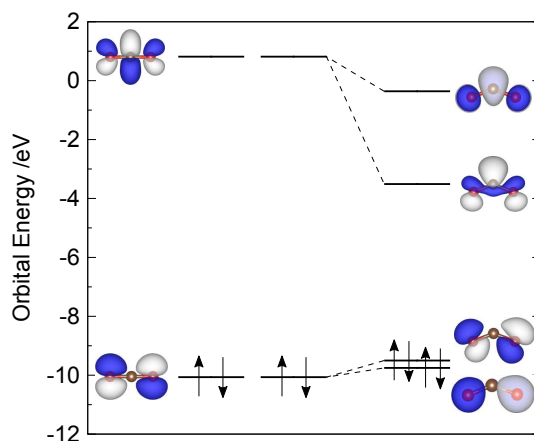


Figure 7: Frontier orbital levels of CO₂ with a linear structure and that extracted from the structure in Figure 6.

-0.03 to 0.48 upon CO₂ adsorption.

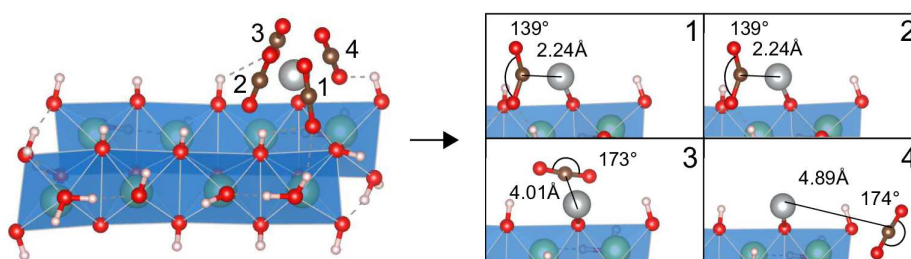


Figure 8: Optimized structures obtained by changing the initial positions of CO₂ such that CO₂ surrounds the Ag atom.

Geometry optimizations are performed by changing the initial positions of CO₂ to examine the dependence of the adsorbed structure. The initial positions of CO₂ are prepared such that CO₂ surrounds the Ag atom where $\Delta\rho(\mathbf{r})$ is distributed. Although $\Delta\rho(\mathbf{r})$ can also be used as a reactivity index, it tends to be delocalized compared to the VCD. Figure 8 shows the optimized structures obtained for each initial CO₂ position. Optimized structures 1 and 2 in Figure 8 are the same as that in Figure 6. In structures 3 and 4, CO₂ has a linear structure that is unfavorable for the reduction of CO₂. Furthermore, the E_{ad} of CO₂ for structures 3 and 4 are calculated to be 0.47 and 0.30 eV, respectively. These values are smaller than the values of E_{ad} for structures 1 and 2 of 0.58 eV. Therefore, the adsorption of CO₂ in the region where the VCD is localized is advantageous for the CO₂ reduction, as well as being the most stable of the optimized structures. Consequently, the regioselectivity of CO₂ adsorption is clearly indicated by the VCD because of the considerations of the vibronic contribution to the stabilization of the system in contrast to $\Delta\rho(\mathbf{r})$, which only considers the electronic contribution. As shown in Figure S3 of the Supplementary Material, the optimized structures obtained by placing CO₂ on Ga atoms are energetically unstable

compared to the structure obtained by the VCD analysis.

5 Conclusion

A cluster model of the Ga_2O_3 photocatalyst surface is constructed by terminating dangling bonds with H atoms. The H atoms are bonded to O atoms with large orbital coefficients for each unoccupied orbitals such that the cluster model has an energy gap in agreement with the experimental values. The O atoms without hydrogen termination act as Lewis bases. This process of building a cluster model for metal oxide surfaces is termed as the step-by-step hydrogen-terminated (SSHT) approach. The vibronic coupling density (VCD) of the Ag-loaded Ga_2O_3 cluster is evaluated to identify the adsorption sites for CO_2 . Thus, the VCD is an effective reactivity index for determining the regioselectivity of CO_2 adsorption on the Ag-loaded Ga_2O_3 surface. We also found that CO_2 with a bent structure, which is advantageous for photocatalytic reduction, is adsorbed on the Ag atom.

Acknowledgments

This work was supported by the Elements Strategy Initiative for Catalysts and Batteries (ESICB). The calculations were partly performed using the Supercomputer Laboratory of Kyoto University and Research Center for Computational Science, Okazaki, Japan.

References

- [1] G. Ertl, H. Knözinger, F. Schüth, J. Weitkamp, Handbook of Heterogeneous Catalysis, 2nd ed., Wiley-VCH, Weinheim, 2008.
- [2] N. Haruta, T. Sato, K. Tanaka, J. Org. Chem. 77 (2012) 9702.
- [3] T. Sato, N. Iwahara, N. Haruta, K. Tanaka, Chem. Phys. Lett. 531 (2012) 257.
- [4] N. Haruta, T. Sato, K. Tanaka, Tetrahedron 70 (2014) 3510.
- [5] N. Haruta, T. Sato, K. Tanaka, J. Org. Chem. 80 (2014) 141.
- [6] N. Haruta, T. Sato, K. Tanaka, Tetrahedron Lett. 56 (2015) 590.
- [7] K. Teramura, H. Tsuneoka, T. Shishido, T. Tanaka, Chem. Phys. Lett. 467 (2008) 191.

- [8] H. Tsuneoka, K. Teramura, T. Shishido, T. Tanaka, *J. Phys. Chem. C* 114 (2010) 8892.
- [9] K. Teramura, Z. Wang, S. Hosokawa, Y. Sakata, T. Tanaka, *Chem. Eur. J.* 20 (2014) 9906.
- [10] Z. Wang, K. Teramura, S. Hosokawa, T. Tanaka, *J. Mater. Chem. A* 3 (2015) 11313.
- [11] Z. Wang, K. Teramura, Z. Huang, S. Hosokawa, Y. Sakata, T. Tanaka, *Catal. Sci. Technol.* 6 (2016) 1025.
- [12] M. Yamamoto, T. Yoshida, N. Yamamoto, T. Nomoto, Y. Yamamoto, S. Yagi, H. Yoshida, *J. Mater. Chem. A* 3 (2015) 16810.
- [13] Y. Kawaguchi, M. Akatsuka, M. Yamamoto, K. Yoshioka, A. Ozawa, Y. Kato, T. Yoshida, *J. Photochem. Photobiol. A* 358 (2018) 459.
- [14] T. Sato, K. Tokunaga, K. Tanaka, *J. Phys. Chem. A* 112 (2008) 758.
- [15] T. Sato, K. Tokunaga, N. Iwahara, K. Shizu, K. Tanaka, in: H. Köppel, D. R. Yarkony, H. Barentzen (Eds.), *Vibronic Coupling Constant and Vibronic Coupling Density in The Jahn-Teller Effect: Fundamentals and Implications for Physics and Chemistry*, Springer-Verlag, Berlin and Heidelberg, 2009.
- [16] R. G. Parr, W. Yang, *J. Am. Chem. Soc.* 106 (1984) 4049.
- [17] R. G. Parr, W. Yang, *Density-Functional Theory of Atoms and Molecules*, Oxford University Press, New York, 1994.
- [18] M. J. Frisch et al., *Gaussian 09, Revision D. 01*, Gaussian, Inc., Wallingford CT, 2013.
- [19] M. J. Frisch et al., *Gaussian 09, Revision E. 01*, Gaussian, Inc., Wallingford CT, 2013.
- [20] S. Geller, *J. Chem. Phys.* 33 (1960) 676.
- [21] J. Åhman, G. Svensson, J. Albertsson, *Acta Cryst. C* 52 (1996) 1336.
- [22] H.-J. Freund, M. W. Roberts, *Surf. Sci. Rep.* 25 (1996) 225.

Supplementary Material
Model Building of Metal Oxide Surfaces and
Vibronic Coupling Density as a Reactivity Index:
Regioselectivity of CO₂ Adsorption on Ag-loaded Ga₂O₃

Yasuro Kojima¹, Wataru Ota^{1,2}, Kentaro Teramura^{1,3}, Saburo Hosokawa^{1,3}, Tsunehiro Tanaka^{1,3},
Tohru Sato^{1,2,3*}

¹ *Department of Molecular Engineering, Graduate School of Engineering, Kyoto University,
Nishikyo-ku, Kyoto 615-8510, Japan*

² *Fukui Institute for Fundamental Chemistry, Kyoto University, Sakyo-ku, Kyoto 606-8103,
Japan*

³ *Unit of Elements Strategy Initiative for Catalysts & Batteries, Kyoto University, Nishikyo-ku,
Kyoto 615-8510, Japan*

(Dated: August 23, 2018)

^{*} Corresponding author at: Fukui Institute for Fundamental Chemistry, Kyoto University, Takano Nishihiraki-cho 34-4 Sakyo-ku, Kyoto 606-8103, Japan.
Email address: tsato@scl.kyoto-u.ac.jp

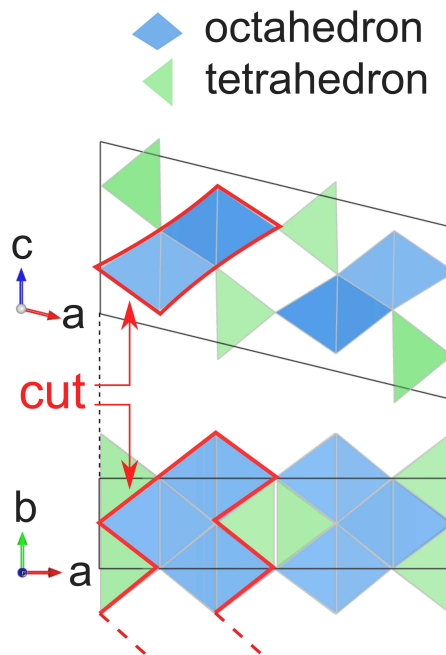


Figure S 1: β -Ga₂O₃ with lattice parameters $a = 12.23\text{\AA}$, $b = 3.04\text{\AA}$, $c = 5.80\text{\AA}$, and $\beta = 103.7^\circ$ [1]. Eight adjacent octahedral sites were used as the cluster model.

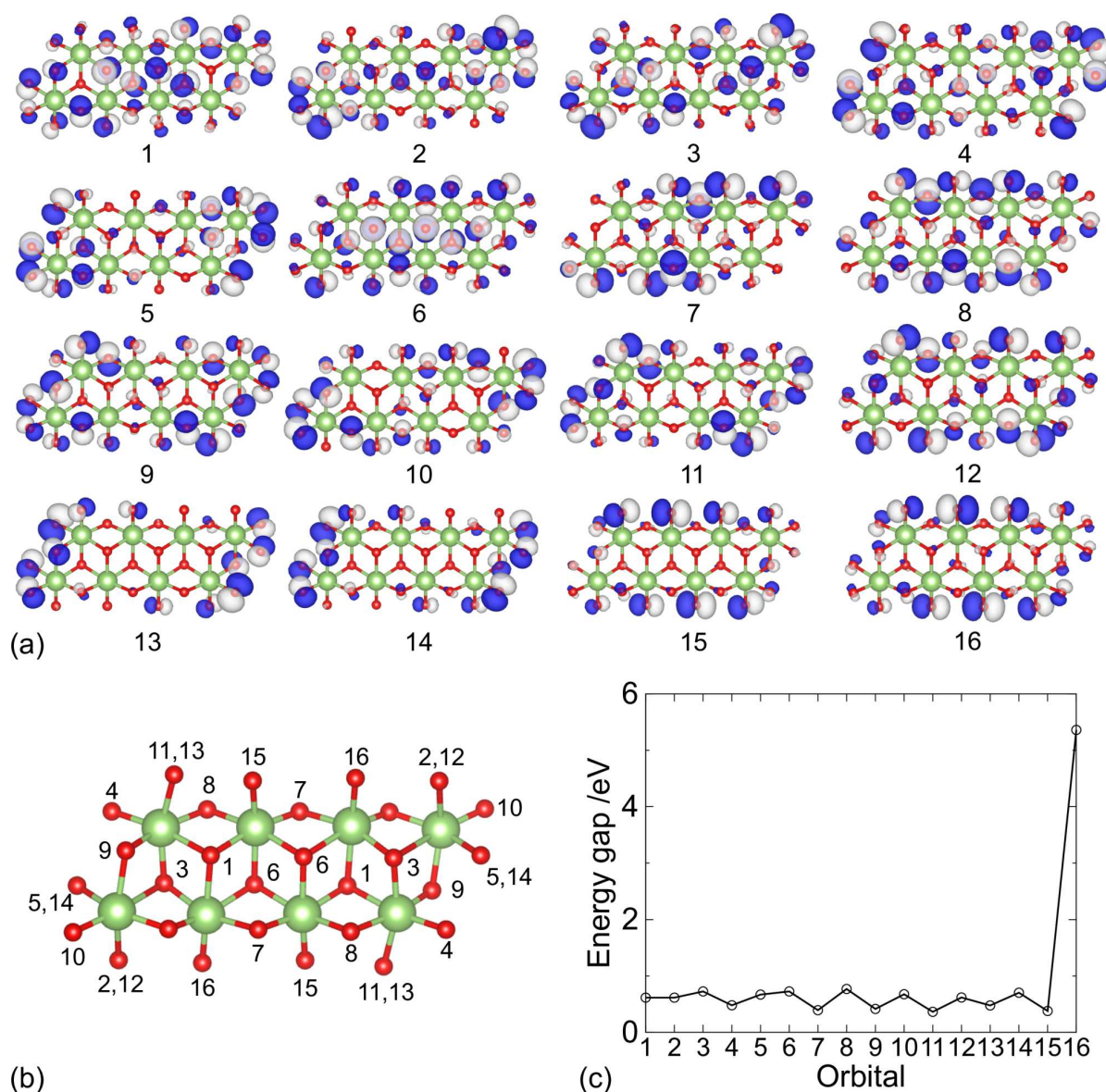


Figure S 2: (a) Orbital coefficients of the unoccupied molecular orbitals of the bare cluster. Numbers are given in ascending order of the orbital energy. The orbital coefficients labeled 1 correspond to the LUMO of the bare cluster. (b) The O atoms with large orbital coefficients for each unoccupied molecular orbitals. Two H atoms were added step-by-step for each orbital. (c) The energy gaps of the H-terminated clusters; these increase when orbital 16 is occupied. The energy gaps were calculated by removing H atoms from the optimized SSHT model. Because the bare cluster consists of 8 Ga and 28 O atoms, the sum of the oxidation numbers in the SSHT model is 0 after the introduction of 32 H atoms if we assume that the oxidation numbers of Ga, O, and H are +3, -2, and +1, respectively.

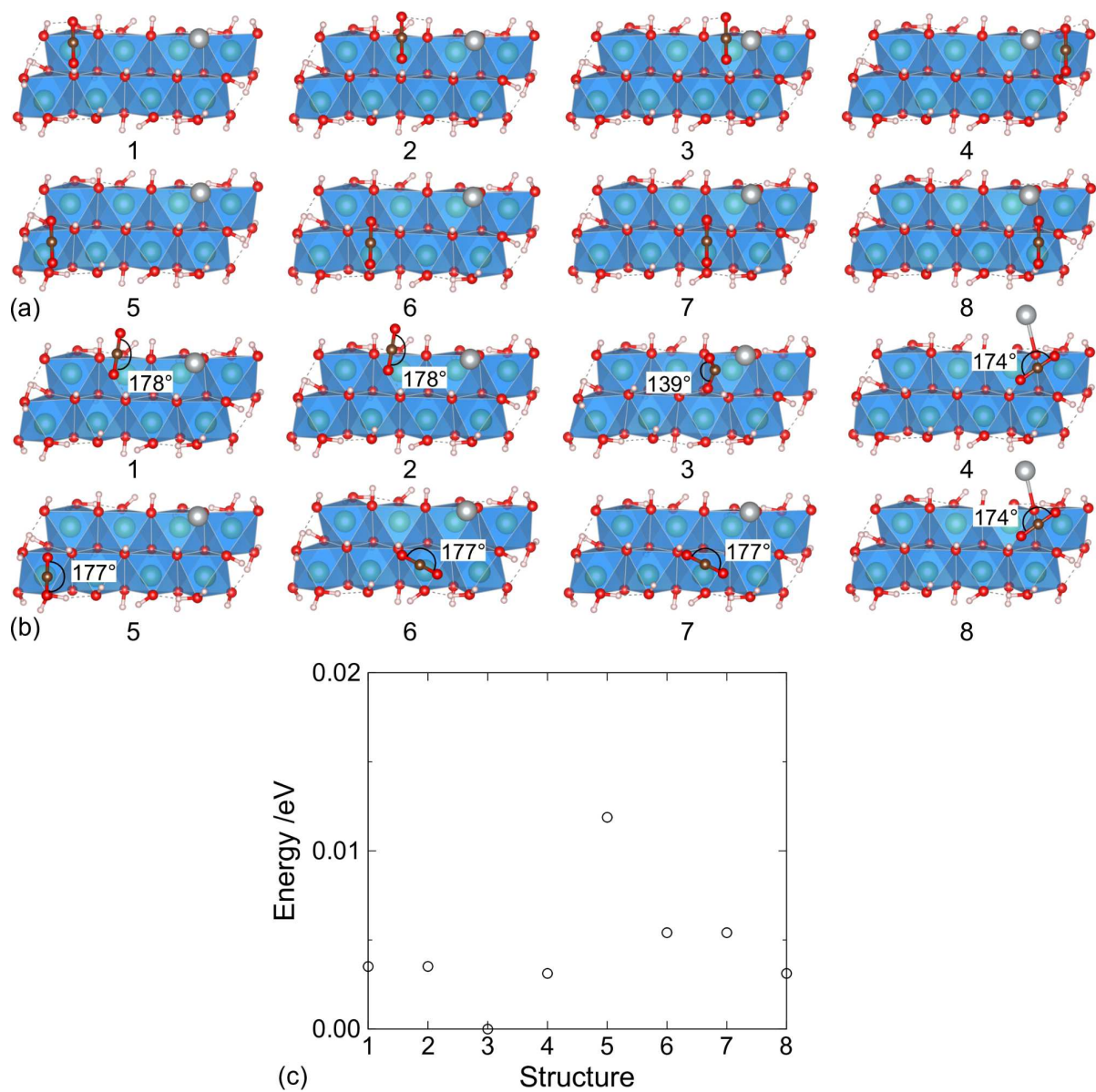


Figure S 3: (a) Initial configurations of CO₂ over the Ag-loaded Ga₂O₃ cluster where CO₂ is placed on the Ga atoms. (b) Optimized structures and the values of the O-C-O angles. (c) Energies of the optimized structures subtracted from that of the structure predicted by VCD. The calculated energy differences are zero for structure 3, which is the same as that predicted by VCD, and positive for the other structures.

Table S 1: Cartesian coordinates (\AA) of the SSHT cluster model for the Ga_2O_3 surface.

No.	Atom	x	y	z	No.	Atom	x	y	z
1	Ga	-5.3237	-0.8058	0.4860	35	O	6.8634	1.3493	-1.3235
2	Ga	-2.4557	-1.1803	0.0074	36	O	5.2737	2.3049	1.0928
3	Ga	0.6034	-1.4413	0.0528	37	H	-2.3809	0.5814	1.7768
4	Ga	3.5952	-1.7169	0.2520	38	H	2.3806	-0.5806	-1.7762
5	Ga	-3.5954	1.7170	-0.2521	39	H	-5.7084	-3.0520	-0.6573
6	Ga	-0.6033	1.4414	-0.0521	40	H	5.7093	3.0523	0.6581
7	Ga	2.4559	1.1801	-0.0061	41	H	-3.5852	-0.0498	-2.1110
8	Ga	5.3241	0.8059	-0.4877	42	H	3.5810	0.0465	2.1123
9	O	-4.9979	2.4166	-1.3014	43	H	-4.7369	2.8743	-2.1082
10	O	-1.9662	2.1832	-1.2603	44	H	4.7394	-2.8780	2.1045
11	O	0.9521	1.8286	-1.1128	45	H	6.4063	0.4370	1.7642
12	O	3.8076	1.5368	-1.1815	46	H	-6.4097	-0.4352	-1.7654
13	O	-3.8080	-1.5367	1.1820	47	H	-0.6458	-0.3062	-1.9339
14	O	-0.9520	-1.8284	1.1139	48	H	0.6443	0.3063	1.9350
15	O	1.9664	-2.1840	1.2606	49	H	-1.1551	-2.7065	1.4561
16	O	4.9990	-2.4167	1.2993	50	H	1.1557	2.7076	-1.4526
17	O	-5.2730	-2.3053	-1.0932	51	H	-1.8420	3.1377	-1.3470
18	O	-2.6127	-2.6522	-1.2060	52	H	1.8421	-3.1388	1.3441
19	O	0.6586	-2.8876	-1.1689	53	H	-5.7097	1.6024	0.9589
20	O	3.1106	-3.3308	-0.9146	54	H	5.7086	-1.6026	-0.9594
21	O	-4.9008	1.0750	1.0385	55	H	6.6073	1.7510	-2.1644
22	O	-2.2019	0.6718	0.8309	56	H	-6.6080	-1.7503	2.1622
23	O	0.7317	0.3336	0.9746	57	H	3.6198	-3.3427	-1.7361
24	O	3.5772	0.0145	1.1510	58	H	-3.6202	3.3411	1.7368
25	O	-3.5778	-0.0151	-1.1498	59	H	-4.2915	-2.5481	-1.1593
26	O	-0.7319	-0.3337	-0.9734	60	H	4.2922	2.5476	1.1593
27	O	2.2015	-0.6715	-0.8304	61	H	2.0967	-3.3029	-1.1390
28	O	4.9001	-1.0747	-1.0393	62	H	-2.0973	3.3026	1.1393
29	O	-6.8635	-1.3497	1.3206	63	H	-5.9264	1.0324	-1.3045
30	O	-6.3660	0.1727	-1.0146	64	H	5.9269	-1.0315	1.3031
31	O	-3.1113	3.3305	0.9150	65	H	-0.1523	-3.4128	-1.1969
32	O	-0.6595	2.8877	1.1698	66	H	0.1507	3.4138	1.1979
33	O	2.6135	2.6524	1.2064	67	H	-2.3074	-2.4901	-2.1072
34	O	6.3659	-0.1715	1.0137	68	H	2.3071	2.4913	2.1074

Table S 2: Cartesian coordinates (Å) of the SSHT cluster model for the Ag-loaded Ga₂O₃ surface.

No.	Atom	x	y	z	No.	Atom	x	y	z
1	Ag	3.4721	0.9901	2.6839	36	O	-7.2861	-1.4287	-0.9215
2	Ga	5.0152	0.5699	-0.4111	37	O	-5.5254	-2.1278	1.4726
3	Ga	2.1368	1.0304	-0.5291	38	H	2.0177	-0.5219	1.4944
4	Ga	-0.9058	1.3851	-0.3358	39	H	-2.8154	0.3464	-1.9205
5	Ga	-3.8739	1.7413	0.0414	40	H	5.4123	2.5685	-1.8446
6	Ga	3.2169	-1.9309	-0.3957	41	H	-6.0009	-2.9146	1.1692
7	Ga	0.2420	-1.5243	-0.1789	42	H	3.3066	-0.3939	-2.4591
8	Ga	-2.7873	-1.1819	0.0537	43	H	-3.6992	0.2321	2.0967
9	Ga	-5.6848	-0.8232	-0.2682	44	H	4.1298	-3.4437	-2.1236
10	O	4.4839	-2.8578	-1.4458	45	H	-4.8714	3.1355	1.8185
11	O	1.5526	-2.4322	-1.3223	46	H	-6.5720	-0.1702	2.0026
12	O	-1.3805	-1.9811	-1.0918	47	H	6.1748	-0.3780	-2.5481
13	O	-4.2244	-1.6538	-0.9690	48	H	0.2242	0.0160	-2.2548
14	O	3.6392	1.5067	0.4331	49	H	-0.8040	-0.1199	1.7345
15	O	0.7329	1.8739	0.5495	50	H	0.9594	2.7516	0.8763
16	O	-2.1660	2.2981	0.8613	51	H	-1.6168	-2.8966	-1.2831
17	O	-5.1896	2.5881	1.0922	52	H	1.3872	-3.3842	-1.3312
18	O	4.8647	1.8188	-2.1216	53	H	-2.0294	3.2545	0.8419
19	O	2.2856	2.2784	-1.9727	54	H	5.4218	-1.6329	0.7432
20	O	-1.0294	2.6581	-1.7372	55	H	-6.0690	1.5225	-0.9928
21	O	-3.4568	3.1884	-1.3476	56	H	-7.1002	-1.9333	-1.7246
22	O	4.6270	-1.0912	0.6387	57	H	6.4974	1.8264	0.8840
23	O	1.8832	-0.6870	0.5391	58	H	-4.0279	3.1172	-2.1242
24	O	-0.9841	-0.2594	0.7959	59	H	3.2559	-3.1095	1.8587
25	O	-3.7963	0.1349	1.1444	60	H	3.8945	2.1306	-2.1252
26	O	3.2922	-0.2994	-1.5006	61	H	-4.5463	-2.3791	1.4924
27	O	0.3703	0.1375	-1.3085	62	H	-2.4654	3.1023	-1.6410
28	O	-2.5688	0.5479	-1.0074	63	H	1.7408	-3.2378	1.2512
29	O	-5.2753	0.9712	-1.0647	64	H	5.4863	-1.6314	-1.7779
30	O	6.6386	1.2583	0.1151	65	H	-6.1247	1.2244	1.3303
31	O	5.9832	-0.7543	-1.6802	66	H	-0.2509	3.2215	-1.8343
32	O	2.7633	-3.2885	1.0451	67	H	-0.5095	-3.2697	1.3902
33	O	0.3263	-2.8264	1.1916	68	H	1.8075	2.0646	-2.7831
34	O	-2.8492	-2.4997	1.4393	69	H	-2.5080	-2.2174	2.2972
35	O	-6.5896	0.3424	1.1826					

References

- [1] S. Geller, J. Chem. Phys. 33 (1960) 676.